



Title	The L12 to DO19 phase transformation in the intermetallic compound Fe₃Ge
Author(s)	Chen, QZ; Ngan, AHW; Duggan, BJ
Citation	The 1997 Materials Research Society Symposium, Boston, MA., 1-5 December 1997. In Conference Proceedings, 1998, v. 481, p. 225-230
Issued Date	1998
URL	http://hdl.handle.net/10722/46646
Rights	Creative Commons: Attribution 3.0 Hong Kong License

THE $L1_2$ TO DO_{19} PHASE TRANSFORMATION IN THE INTERMETALLIC COMPOUND Fe_3Ge

Q.Z. CHEN *, A.H.W. NGAN **, B.J. DUGGAN **

* Department of Materials Physics, University of Science and Technology Beijing, Beijing 100083, P.R. China

** Department of Mechanical Engineering, The University of Hong Kong, Pokfulam Road, Hong Kong

ABSTRACT

A large kinetics hysteresis is found to exist between the forward and backward reactions of the $L1_2 \leftrightarrow DO_{19}$ transformation in Fe_3Ge . The slow DO_{19} to $L1_2$ transformation leaves behind very stable twins and stacking fault debris. *In-situ* annealing experiments in the transmission electron microscope revealed that nucleation for the reverse $L1_2$ to DO_{19} reaction takes place efficiently at these defects.

INTRODUCTION

The $L1_2$ to DO_{19} transformation is known to take place in a few A_3B ordered intermetallic compounds including Fe_3Ge , Fe_3Ga , Ga_3Tb , Tl_3Bi and Zn_3Mn . From a crystallographic viewpoint, the $L1_2$ to DO_{19} transformation happens via shear on every other $\{111\}$ plane of the parent $L1_2$ crystal by the $1/3\langle 112 \rangle$ vector, thus converting the packing sequence from ...abcabc... for $L1_2$ into ...ababab... for DO_{19} . The situation is therefore analogous to that in the fcc to hcp transformation in disordered systems, except that the shear vector is now $1/3\langle 112 \rangle$ rather than the usual $1/6\langle 112 \rangle$ Shockley for the disordered case. Unlike the well-documented fcc to hcp transformation, however, little is known about the kinetics characteristics and dislocation level mechanism in the $L1_2$ to DO_{19} transformation. In this work, we have studied the transformation kinetics of both the forward and backward reactions of the $L1_2 \leftrightarrow DO_{19}$ transformation in Fe_3Ge , and have performed *in-situ* annealing experiments in the transmission electron microscope (TEM) to characterise the dislocation mechanisms responsible for the forward $L1_2$ to DO_{19} reaction. Fig. 1 below shows the phase diagram of the Fe-Ge system.

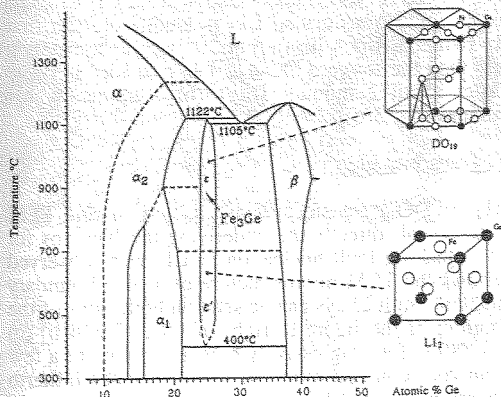


Fig. 1 - Phase Diagram of the Fe-Ge system, showing the $L1_2$ to DO_{19} transformation at around the Fe_3Ge composition.

EXPERIMENTAL

An Fe₃Ge ingot was prepared by arc-melting under an argon atmosphere followed by remelting several times to achieve macroscopic homogeneity. The composition was confirmed by energy dispersive analysis to be Fe₇₅Ge₂₅. Transformation heat treatments were performed on small blocks (about 4 × 4 × 3 mm³) cut from the as-cast ingot. The relative volume fractions of the parent and daughter phases were revealed by a crystallographic etching technique using 67% HF + 33% H₂O₂, and the phases were identified in the scanning electron microscope by electron back-scattered diffraction (EBSD). TEM preparation was performed using the same conditions as reported earlier [1]. TEM observations were made on a JEM 2000FX operating at 200 kV. *In-situ* annealing experiments were performed using an Oxford double-tilt heating stage at 780°C which was close to the operation limit of 800°C of the stage.

RESULTS

Overall Transformation Kinetics

Fig. 1 indicates that the transformation between L1₂ and DO₁₉ takes place at about 700°C. The as-cast microstructure of the ingot was confirmed by EBSD to consist of predominantly DO₁₉ phase with a small volume fraction of the B2 phase [fig. 2(a)]. Fig. 2(b)-(f) shows the quenched microstructures after heating the as-cast microstructure at 600°C for different times. EBSD analyses indicated that the B2 phase had transformed independently into the B8₁ phase. Within the DO₁₉ phase, dense strips, which were not present hitherto in the as-cast microstructure, appeared after about 1 day at 600°C [fig. 2(b)]. These strips were confirmed by TEM to be stacking fault bundles in the DO₁₉ matrix and hence embryos of the daughter L1₂ phase. Upon further heating, the strip density gradually increased [fig. 2(b)-(d)], and well-formed islands of L1₂ also began to emerge [fig. 2(c) - (d)]. The overall speed of the transformation was very slow, taking some 30 days to complete [fig. 2(f)]. It should be noted that the newly formed L1₂ grains contained relatively few twins [fig. 2(c)-(d)], but upon further heating, the previously transformed L1₂ phase gradually became heavily twinned [fig. 2(e)-(f)]. These twins are extremely difficult to get rid of even after prolonged heating at temperatures in the L1₂ phase field [1]. Transformation experiments have also been performed at 695°C, which is even closer to the equilibrium temperature of 700°C. It was found that the transformation kinetics from DO₁₉ to L1₂ was even slower than that at 600°C. For example, a specimen heat treated at 695°C for eight days contained no well-formed L1₂ grains and much sparser stacking fault strips than what is shown in fig. 2(c) & (d).

Fig. 3 shows the microstructural changes for the reverse transformation from L1₂ to DO₁₉ at 705°C. The starting microstructure was the fully transformed L1₂ product from the first DO₁₉ to L1₂ reaction and was thus heavily twinned. Upon heating at 705°C, transformation back to DO₁₉ took place much more rapidly than the forward DO₁₉ to L1₂ reaction, as fig. 3 shows. The first DO₁₉ grains appeared after about 2 minutes [fig. 3(b)], and the whole transformation completed in just about 5 minutes [fig. 3(d)].

Dislocation Mechanism for the L1₂ to DO₁₉ Transformation

The much quicker kinetics of the L1₂ to DO₁₉ transformation enabled *in-situ* TEM annealing experiments to be carried out to reveal directly the underlying mechanisms for the reaction. Three distinct mechanisms of stacking fault nucleation in L1₂ were observed and these are described below. Fig. 4(a) shows the TEM microstructure of a twin boundary area of the starting L1₂ phase. Numerous stacking fault arrays can be seen on both sides of the twin boundary, which runs from the left bottom of the figure to right middle. Fig. 4(b)-(c) show the same area after *in-situ* annealing at 780°C for progressively longer times up to a few hours. It can be seen that faulting into a "stair-rod" configuration had taken place at a hitherto screw dislocation site (pointed at by a white arrow in fig. 4(b)). Faulting into the twin matrix can also be seen to originate frequently along the twin boundary. Fig. 5 shows a thicker area after prolonged heating at 780°C. In this micrograph, the stacking fault array which runs

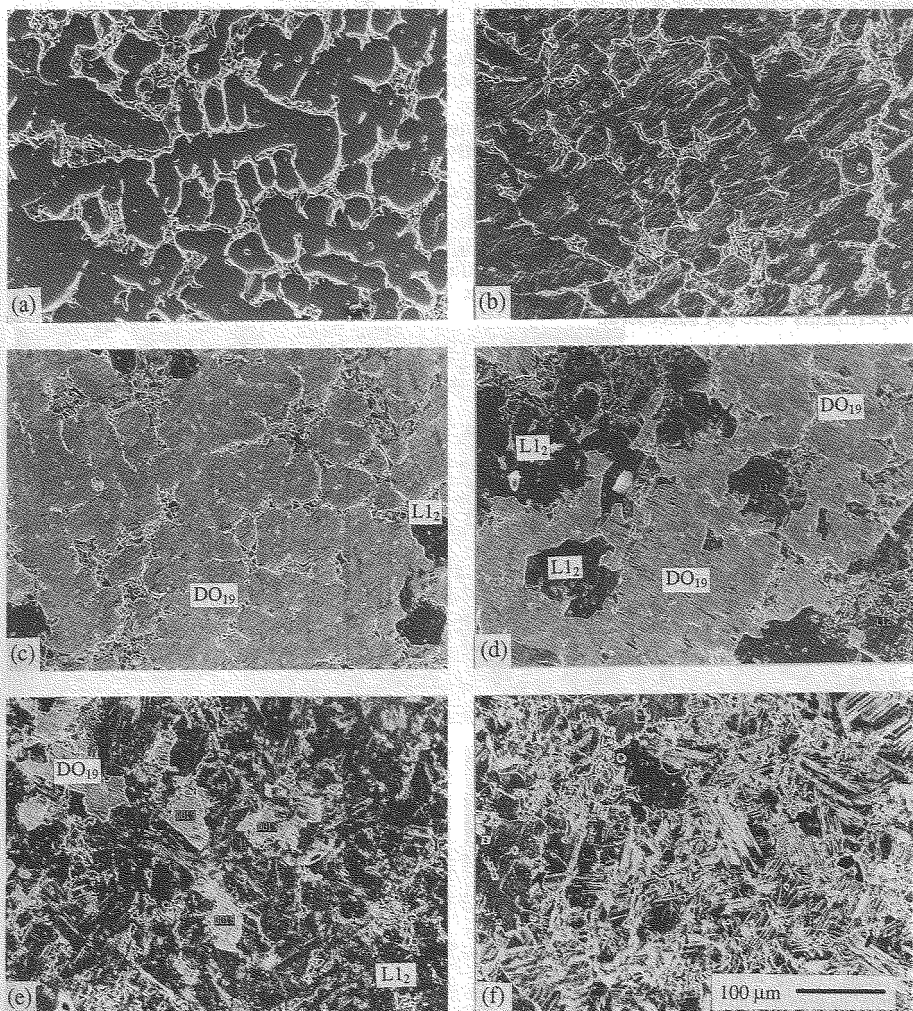


Fig. 2 - (a) The initial microstructure of Fe₃Ge showing the predominant DO₁₉ (the darker) phase and a small volume fraction of B2 (the lighter) phase. (b)-(f) Quenched microstructures after heat treating the microstructure in (a) at 600°C for (b) 1 day, (c) 6 days, (d) 10 days, (e) 20 days and (f) 30 days. All micrographs have same magnification.

diagonally across the figure was debris left-behind in the starting $L1_2$ phase due to the previous DO_{19} to $L1_2$ transformation. Upon *in-situ* heating at 780°C , new stacking faults can be seen to overlap on these existing ones. The mechanism involves the formation of "stair-rod" defects; one arm of the stair-rod grew at high speed to overlap an existing stacking fault bundle, the other arm grew much slowly into the open parent matrix. It is interesting to note that all the newly grown stacking faults in figs. 4 and 5 had round heads, indicating that a negative stacking fault energy was pushing against surface drag.

The observations here indicate that DO_{19} embryos in the form of stacking faults can nucleate in the $L1_2$ matrix by at least three mechanisms, i.e. formation of stair-rod defects from residual dislocations, nucleation directly from the numerous twin boundaries, and overlapping on existing stacking faults. Image simulation on the leading edges of the newly formed stacking faults showed that they were not simple $-1/3\langle 112 \rangle$ super-Shockley partials [2]. The observation here is therefore very different from the common mechanism observed in the ordinary fcc to hcp transformation, which involves extensive glide activities leading to Shockley dissociation by interaction with existing dislocations or stacking faults [3].

The backward DO_{19} to $L1_2$ reaction is very sluggish and hence *in-situ* annealing experiments were not successful.

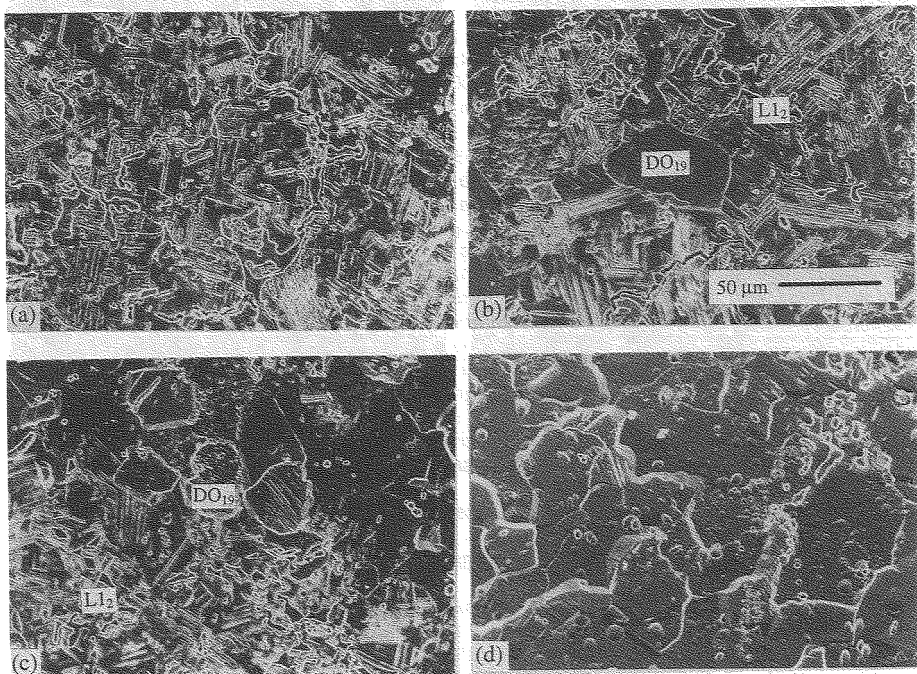


Fig. 3 - Quenched microstructure of Fe_3Ge after heat treatment the $L1_2$ phase at 705°C for (a) 105 sec, (b) 110 sec, (c) 120 sec and (d) 300 sec. All micrographs have the same magnification

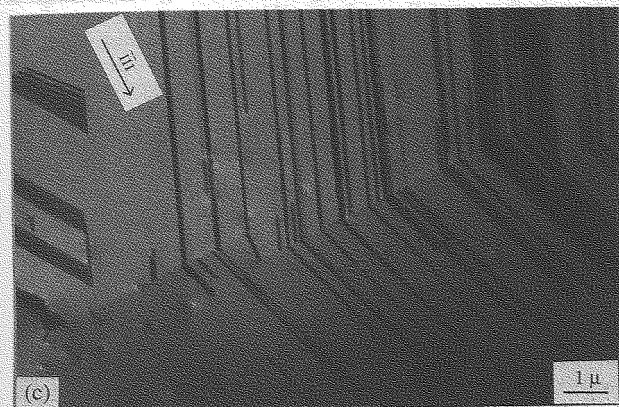
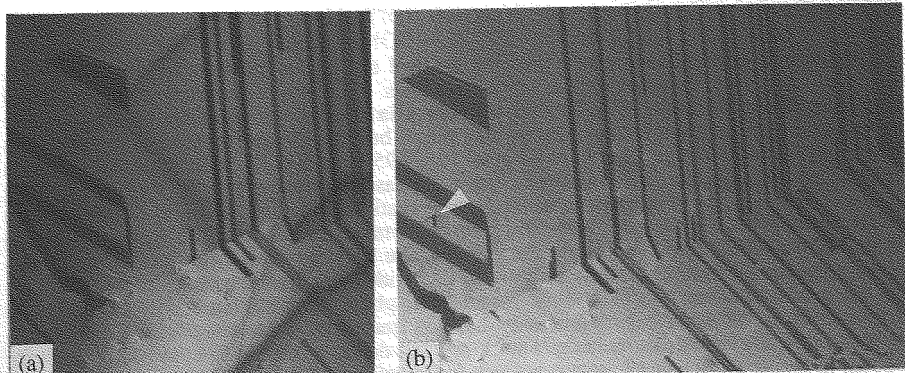


Fig. 4 -
TEM micrographs
showing stacking fault
growth in $L1_2$ during *in-situ*
annealing.
(a) Before annealing. (b)-
(c) After annealing at
780°C for progressively
longer times.

Fig. 5 -
TEM micrograph of a
thick area showing
stacking fault overlapping
after *in-situ* annealing at
780°C.



DISCUSSION

The results here indicate clearly that the forward and backward transformations between $L1_2$ and DO_{19} in Fe_3Ge exhibit a large hysteresis. This hysteresis cannot be explained satisfactorily by simply considering the difference in thermal agitation for the temperature ranges in which the two transformations take place, because the transformation temperatures chosen in the present study were not far apart (e.g. $695^\circ C$ vs $705^\circ C$). A more probable reason for the hysteresis is the low stability of the $L1_2$ phase with respect to faulting or twinning below $700^\circ C$ [1]. This is evident from the observation that newly formed $L1_2$ grains are relatively twin free but upon prolonged heating at temperatures below $700^\circ C$, they twin and fault heavily. This does not only imply that the driving force for the DO_{19} to $L1_2$ transformation is small, for a low stability of $L1_2$ with respect to twinning and faulting also means low stability with respect to the parent DO_{19} phase, but also that the forward DO_{19} to $L1_2$ reaction would leave behind a heavily defected starting microstructure for the reverse $L1_2$ to DO_{19} reaction. The dense twins and stacking fault debris left behind in the $L1_2$ phase were shown to be very efficient nucleation sources for transforming back into DO_{19} when heated at above $700^\circ C$. It is interesting to note that crystallography would prevent the reverse from happening. Twinning is not allowed in DO_{19} , and even though stacking faults may occur in DO_{19} , they are not as efficient as nucleation sites for $L1_2$ as are the stacking faults in $L1_2$ for DO_{19} . This is because there are three non-parallel close-packed planes intersecting a given stacking fault in the $L1_2$ structure for DO_{19} nuclei to form, but there is no close-packed plane intersecting a stacking fault in DO_{19} for $L1_2$ nuclei. The *in-situ* annealing results here suggest that this crystallographic factor is the main reason for the much quicker kinetics for the $L1_2$ to DO_{19} transformation in Fe_3Ge .

CONCLUSION

A large hysteresis exists in the transformation between the $L1_2$ and DO_{19} phase in Fe_3Ge . The DO_{19} to $L1_2$ reaction is much slower than the reverse reaction. This is thought to be due to the low stability of the $L1_2$ phase with respect to twinning and fault, thus providing a heavily defected starting microstructure for the transformation into DO_{19} . *In-situ* annealing experiments revealed that the numerous twin boundaries and stacking fault debris left in the $L1_2$ phase act as efficient nucleation site for transformation into DO_{19} .

ACKNOWLEDGEMENTS

This work was supported by research grants CRCG #337/064/0037 from HKU and M951006 from the State Key Laboratory for Solid State Microstructures of Nanjing University. Attendance at this conference was sponsored by a conference grant for teachers from HKU. QZC was also supported by a HKU Postdoctoral Fellowship.

REFERENCES

- [1] A.H.W. Ngan, I.P. Jones and R.E. Smallman, *Phil. Mag. A*, **65**, p. 1003 (1992).
- [2] Q.Z. Chen, A.H.W. Ngan and B.J. Duggan, *Intermetallics*, in press.
- [3] H. Fujita and S. Ueda, *Acta Metall.*, **20**, p. 759 (1972).